Bioconjugate Chemistry

Article

pubs.acs.org/bc

Photomodulation of G Protein-Coupled Adenosine Receptors by a Novel Light-Switchable Ligand

María Isabel Bahamonde,[†] Jaume Taura,[‡] Silvia Paoletta,[§] Andrei A. Gakh,[§] Saibal Chakraborty,[§] Jordi Hernando,[¶] Víctor Fernández-Dueñas,[‡] Kenneth A. Jacobson,*[,§] Pau Gorostiza,*[,†,ψ,∥] and Francisco Ciruela*[,‡]

[†]Institute for Bioengineering of Catalonia (IBEC), 08028 Barcelona, Spain

[‡]Unitat de Farmacologia, Departament Patologia i Terapèutica Experimental, Facultat de Medicina, IDIBELL, Universitat de Barcelona, L'Hospitalet de Llobregat, 08907 Barcelona, Spain

[§]Molecular Recognition Section, Laboratory of Bioorganic Chemistry, National Institute of Diabetes and Digestive and Kidney Diseases, National Institutes of Health, Bethesda, Maryland 20892, United States

[¶]Departament de Química, Universitat Autònoma de Barcelona, Cerdanyola del Vallès, 08193 Barcelona, Spain

[ψ]Institució Catalana de Recerca i Estudis Avançats (ICREA), 08010 Barcelona, Spain

[∥]Centro de Investigación Biomédica en Red en Bioingeniería, Biomateriales y Nanomedicina (CIBER-BBN), 50118 Zaragoza, Spain

Supporting Information

ABSTRACT: The adenosinergic system operates through G protein-coupled adenosine receptors, which have become promising therapeutic targets for a wide range of pathological conditions. However, the ubiquity of adenosine receptors and the eventual lack of selectivity of adenosine-based drugs have frequently diminished their therapeutic potential. Accordingly, here we aimed to develop a new generation of light-switchable adenosine receptor ligands that change their intrinsic activity upon irradiation, thus allowing the spatiotemporal control of receptor functioning (i.e., receptor activation/inactivation dependent on location and timing). Therefore, we synthesized an orthosteric, photoisomerizable, and nonselective adenosine receptor agonist, nucleoside derivative MRS5543 containing an aryl diazo linkage on the N^6 substituent, which in the dark (relaxed isomer) behaved as a full adenosine A_3 receptor (A_3R) and partial adenosine A_{2A} receptor ($A_{2A}R$) agonist. Conversely, upon photoisomerization with blue light (460 nm), it remained a full A_3R agonist but became an $A_{2A}R$ antagonist. Interestingly, molecular modeling suggested that structural differences encountered within the third extracellular loop of each receptor could modulate the intrinsic, receptor subtype-dependent, activity. Overall, the development of adenosine receptor ligands with photoswitchable activity expands the pharmacological toolbox in support of research and possibly opens new pharmacotherapeutic opportunities.

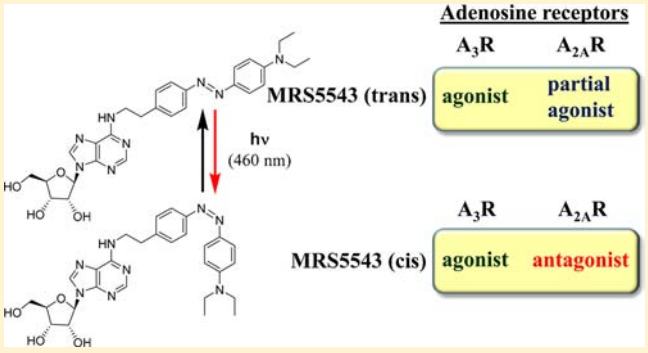

INTRODUCTION

Adenosine, a well-known neuromodulator,[1] exerts its physiological effects through four subtypes (A_1, A_{2A}, A_{2B}, and A_3) of G protein-coupled receptors (GPCRs).[2] Agonists and antagonists of adenosine receptors have an enormous therapeutic potential for both peripheral and central diseases, including cerebral and cardiac ischemic diseases, sleep disorders, immune and inflammatory disorders, Parkinson's disease, epilepsy, and cancer.[3] However, although medicinal chemistry for adenosine receptors has been widely developed in recent decades, several adenosine receptor ligands that entered clinical trials have elicited undesirable side effects precluding their further development. Thus, the in vivo lack of drug selectivity may lead to the inability of controlling receptor activity in time and space. Interestingly, these kinds of drawbacks can be addressed by means of photoisomerization, which for instance was used as the basis to achieve temporal and local activation of biologically active substances or their release from liposomes.[4,5] Similarly, aryl diazo derivatives were designed to interconvert between *cis* and *trans* forms upon irradiation with UV-A light in order to produce differential effects on ion channels, such as potassium channels.[4,5] Azobenzene-based photoswitches have also been used to control metabotropic glutamate receptors at their orthosteric[6] and allosteric[7] sites. Overall, controlling drug activity with light offers the possibility of enhancing pharmacological selectivity with spatiotemporal patterns of

Received: July 25, 2014
Revised: September 22, 2014
Published: September 23, 2014

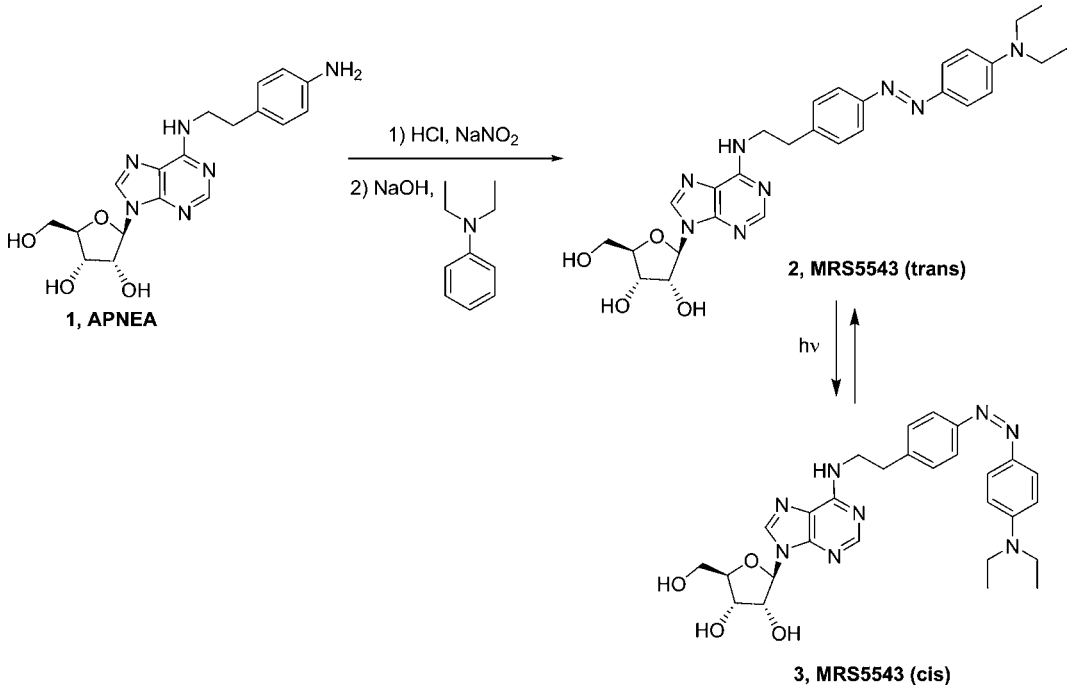

Figure 1. Synthesis of MRS5543, **2**. The photocommutable nucleoside MRS5543 was synthesized in two steps using the nonselective adenosine receptor agonist APNEA **1**, an arylamine that could be readily diazotized without the use of protecting groups.

illumination, thus enabling localized drug effects and the application of dosing patterns.[8]

We now describe a photoswitchable aryl diazo derivative of a potent but nonselective adenosine receptor agonist N^6-2-(4-aminophenyl)ethyladenosine (APNEA **1**), termed MRS5543 **2** (Figure 1), which functions as a photochromic adenosine receptor ligand showing differential pharmacodynamics. The design approach was based on the observation that the N^6 region of adenosine agonists can accommodate diverse substitutions without losing the ability to bind to the receptors, while marked effects on the pharmacological profile, either subtype selectivity or efficacy at a given subtype, are observed following relatively subtle structural changes of the N^6 substituent.[9] Interestingly, X-ray crystallographic analysis of agonist- and antagonist-bound states of the $A_{2A}R$ indicated a conformational reorganization of the second and third extracellular loops (ELs) in an agonist-bound, active-like state.[8] Hydrophobic N^6 substituents of adenosine receptor agonists interact largely with these regions of the receptor. Thus, we hypothesized that the introduction of a *trans*−*cis* photoisomerizable azobenzene group fused with a sterically bulky and extended N^6 chain would have characteristic effects on the agonist profile. Furthermore, in view of potential physiological applications, the photochromic group of MRS5543 was designed to present a red-shifted absorption spectrum with respect to regular, violet-excitable azobenzene and a short-lived *cis* state in aqueous medium that could rapidly back-isomerize to the initial *trans* isomer in the absence of illumination.[10] Overall, here we aimed to demonstrate that photoinduced differential pharmacological responses of this compound could be attained using visible light and a single irradiation source.[11]

RESULTS

MRS5543 Synthesis and Photochemical Characterization. The aryl diazo derivative MRS5543 was prepared from commercially available APNEA and purified to homogeneity using a modification of previously reported methods.[12] In brief, the aryl amine of APNEA was diazotized and the resulting diazonium salt coupled to *p*-(diethylamino)-benzene (Figure 1). Subsequently, we undertook the photochemical characterization of MRS5543 in solution. First, the steady-state absorption spectra of this compound in DMSO and HBSS were measured (Figure 2A). They present similar maxima at λ = 430 (DMSO) and 460 nm (HBSS) arising from the well-known $\pi \rightarrow \pi^*$ transition of its *trans*-azobenzene moiety, which is bathochromically shifted with respect to violet-excitable, regular azobenzenes owing to the diethylamino substituent introduced.[13] As such, *trans* → *cis* photoisomerization of MRS5543 should take place under irradiation with blue-green visible light. However, no azobenzene photoisomerization was observed by steady-state UV−vis absorption spectroscopy upon illumination at λ_{exc} = 420−460 nm in DMSO and HBSS. This was ascribed to the short lifetime expected for the photoinduced *cis* state of the compound due to the azobenzene diethylamino substituent,[11,13] which would therefore lead to fast, spontaneous *cis* → *trans* back-isomerization in the dark.

Transient absorption measurements were conducted to dissect this process. As shown in Figure 2, pulsed excitation of MRS5543 at λ_{exc} = 460 nm in DMSO and HBSS resulted in an immediate loss of *trans* state absorption at λ = 440 nm, thus indicating the formation of the *cis* isomer of the switchable molecule. Because of the lower extinction coefficient of this species within the 380−500 nm region with respect to the *trans* state,[11,13] the transient absorption spectra at t = 0 shows a large negative bleaching signal that mirror-images the steady-state absorption spectra of *trans*-MRS5543 (Figure 2B). Once produced, the *cis* isomer of the compound rapidly returned to the *trans* state via thermal back-isomerization, which allowed the initial absorption at λ = 440 nm to be recovered in the second (in DMSO) and subsecond (in HBSS) time scales, as shown in Figure 2C,D. Thermal *cis* state lifetimes were

dx.doi.org/10.1021/bc5003373 | *Bioconjugate Chem.* 2014, 25, 1847−1854

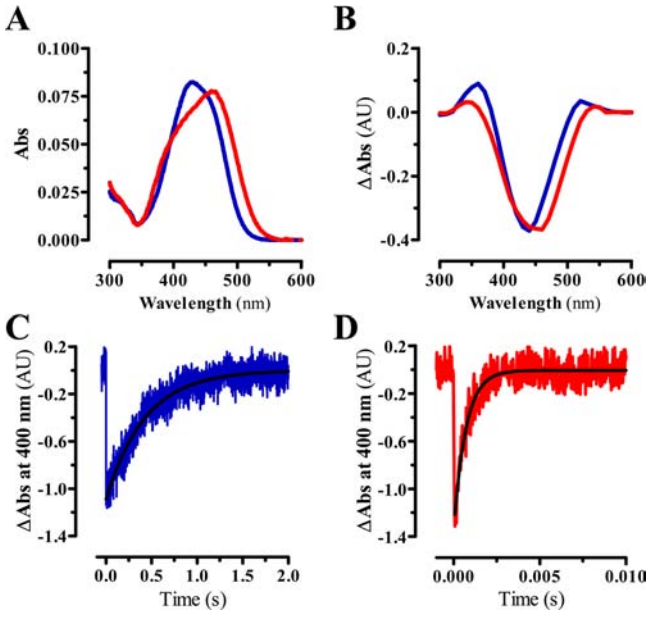

Figure 2. Photochemical characterization of MRS5543. (A) Steady-state absorption spectra of *trans*-MRS5543 (5 μM) in DMSO (blue) and HBSS (red). (B) Transient absorption spectrum at t = 0 of *trans*-MRS5543 (10 μM) upon pulsed excitation at λ_{exc} = 460 nm and 25 °C (DMSO: blue; HBSS: red). (C,D) Variation of the absorption at λ = 440 nm of *trans*−*cis* mixtures of MRS5543 prepared by irradiation of the intitial *trans* state (10 μM) with a single ns laser pulse (t = 0) at λ_{exc} = 460 nm and 25 °C (C: DMSO; D: HBSS). Solid thick lines correspond to monoexponential fitting of the experimental data.

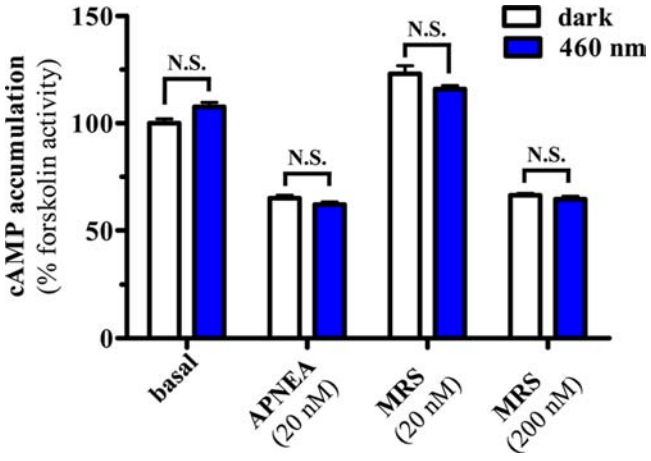

Figure 3. Effect of MRS5543 in A_3R-mediated cAMP accumulation. HEK293 cells were transiently transfected with the human A_3R and the forskolin-stimulated cAMP production was measured in the absence (basal) or presence of APNEA (20 nM), MRS5543 (20 nM), or MRS5543 (200 nM) both in dark conditions (white column) and upon irradiation at 460 nm (purple column). Data (means ± SEM of triplicates) are given as percentage of the forskolin stimulated cells in basal and dark conditions. No significant differences were found when dark vs 460 nm conditions were compared within each treatment (two-way ANOVA with a Bonferroni posthoc test). N.S., not significant. Similar results were obtained in three independent experiments.

determined from monoexponential fits of the experimental absorption recovery curves (τ = 430 and 0.70 ms in DMSO and HBSS, respectively) and they were in agreement with those reported for similar azobenzene systems in polar media.[11,14] Such short lifetimes should enable photodriving the system with a single irradiation source, since the photoinduced *cis* molecules should immediately relax back to their *trans* state when switching off the illumination.

Light-Mediated Modulation of MRS5543 Intrinsic Activity. Once the capability of MRS5543 to photoisomerize was demonstrated, we aimed to assess the ability of both *cis* and *trans* isomers to modulate adenosine receptor functioning. Since we used APNEA (a nonselective adenosine receptor agonist initially used to characterize the A_3R[15]) as the chemical template for the synthesis of MRS5543, it was necessary to evaluate its intrinsic activity at this $G_{\alpha i/o}$ coupled adenosine receptor subtype.[16] Therefore, we assessed A_3R-mediated inhibition of adenylyl cyclase activity upon MRS5543 challenge both in the dark (i.e., *trans* isomer) and during *cis* photoconverting conditions (i.e., continuous 460 nm irradiation). Both isomers of MRS5543 were equally able to inhibit forskolin-induced cAMP accumulation to the same extent as APNEA (Figure 3). Indeed, *cis* and *trans* MRS5543 showed similar potency (EC_{50}) and efficacy (E_{max}) values in modulating adenylyl cyclase activity in cells expressing A_3R (Table 1), thus suggesting that MRS5543 photoisomerization did not alter its A_3R agonist efficacy.

Next, we aimed to study the intrinsic activity of MRS5543 at a different APNEA-sensitive adenosine receptor, the A_{2A}R. Thus, under the same experimental conditions MRS5543 dose-dependently induced cAMP accumulation in dark conditions (EC_{50} = 150 ± 50 nM) (Table 1), indicating a partial agonist behavior when compared to APNEA-mediated full activation of the A_{2A}R (Figure 4, Table 1). Unexpectedly, when A_{2A}R-expressing cells were continuously irradiated at 460 nm (i.e., *cis* photoconverting conditions), MRS5543 was unable to trigger activation of the A_{2A}R (Figure 4) (Table 1). Hence, these results demonstrated that while the *trans* isomer partially activated the A_{2A}R, the *cis* isomer was inactive.

Subsequently, we aimed to elucidate the lack of intrinsic activity of the *cis* MRS5543 isomer. Thus, the potential neutral competitive antagonist activity of this molecule was evaluated. To this end, the ability to compete with a prototypical, orthosteric A_{2A}R full agonist, 2-[*p*-(2-carboxyethyl)phenylethylamino]-5′-*N*-ethylcarboxamidoadenosine (CGS21680), was assessed. Interestingly, when A_{2A}R expressing cells were challenged with CGS21680, cAMP accumulation was observed under both dark and irradiating conditions (Figure 5). This A_{2A}R agonist intrinsic activity was blocked by 4-[2-[7-amino-2-(2-furyl)-1,2,4-triazolo[1,5-*a*][1,3,5]triazin-5-yl-amino]ethyl]-phenol (ZM241385), a selective A_{2A}R antagonist (Figure 5). On the other hand, incubation of cells with CGS21680 plus MRS5543 in the dark (i.e., *trans* MRS5543, partial agonist) prompted a partial A_{2A}R activation, while under *cis* photoconverting conditions MRS5543 was able to completely block CGS21680-mediated cAMP accumulation. These results suggested that the *trans* MRS5543 (i.e., partial agonist) would in fact act as a limited competitive A_{2A}R antagonist in the presence of a full agonist (i.e., CGS21680), thus reducing the potency of CGS21680 with a concomitant net decrease in the activation of the A_{2A}R, and importantly confirming that the *cis*-isomer behaved purely as a competitive antagonist (Figure 5). Overall, we concluded that both MRS5543 isomers showed agonist activity at the A_3R while the *cis* and *trans* isomers of MRS5543 showed antagonist and partial agonist activity at the A_{2A}R, respectively.

dx.doi.org/10.1021/bc5003373 | *Bioconjugate Chem.* 2014, 25, 1847−1854

Table 1. Half-Maximal-Effective Concentration (EC_{50}) Values and Maximum Responses (E_{max}) of APNEA and MRS5543 Modulating Adenylyl Cyclase Activity in Transfected HEK293 Cells Expressing the Indicated Adenosine Receptor[b]

		Adenosine Receptor			
		A_3R		$A_{2A}R$	
Ligand	APNEA	EC_{50} (nM) 20±2.5 E_{max} 100±9.1	EC_{50} (nM) 17±5.4 E_{max} (% dark) 108±9	EC_{50} (nM) 34±17 E_{max} 100±10.4	EC_{50} (nM) 23±13 E_{max} (% dark) 84±11.7
	MRS5543	EC_{50} (nM) 119±11.8 E_{max} (% APNEA) 100±3.5	EC_{50} (nM) 118 ±13.6 E_{max} (% APNEA) 90±7.6	EC_{50} (nM) 150±50 E_{max} (% APNEA) 64±8[a]	EC_{50} (nM) N.D. E_{max} (% APNEA) N.D.
		dark	460 nm	dark	460 nm

[b]The maximal efficacy (E_{max}) of MRS5543 in modulating adenylyl cyclase activity through the A_3R and $A_{2A}R$ is compared to that observed for APNEA. Also, for each compound (i.e., APNEA and MRS5543) the impact of 460 nm irradiation into the EC_{50} and E_{max} was analyzed. N.D. non determinable. [a]$P < 0.05$ vs APNEA.

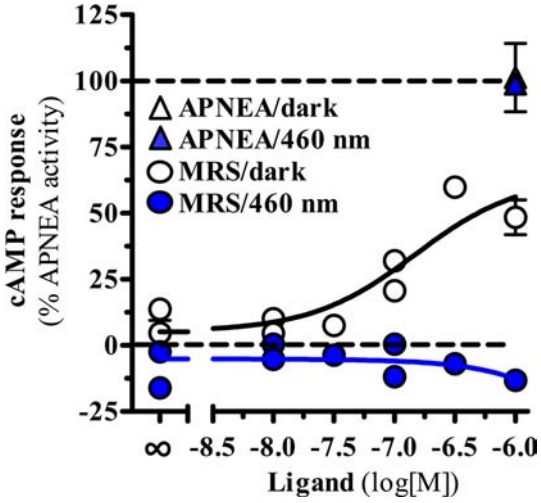

Figure 4. MRS5543-dependent photomodulation of $A_{2A}R$-mediated cAMP accumulation. HEK293 cells were transiently transfected with the human $A_{2A}R$ and the cAMP production was measured in the absence or presence of increasing concentrations of MRS5543 both in dark conditions (white circles) and upon irradiation at 460 nm (purple circles). APNEA (1 μM) was used as a positive control of $A_{2A}R$-mediated cAMP accumulation. Data (means ± SEM of triplicates) are given as fold over the basal activity. Similar results were obtained in three independent experiments.

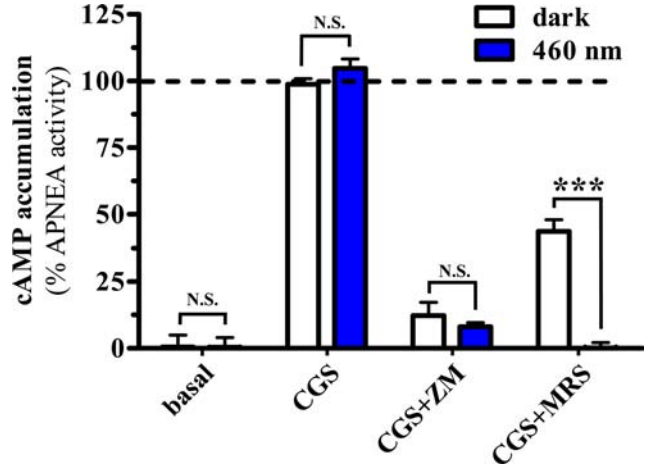

Figure 5. MRS5543 *cis* isomer blocks $A_{2A}R$-mediated cAMP accumulation. HEK293 cells were transiently transfected with the human $A_{2A}R$ and the cAMP production was measured upon stimulation with the $A_{2A}R$ agonist CGS21680 (500 nM) alone or in the presence of ZM241385 (1 μM) or MRS5543 (3 μM) both in dark conditions (white columns) and upon irradiation at 460 nm (purple columns). Data (means ± SEM of triplicates) are given as percentage of the CGS stimulated cells in dark conditions. The asterisks denote data significantly different when dark vs 460 nm was compared. ***$P < 0.001$, two-way ANOVA with a Bonferroni posthoc test. N.S., not significant. Similar results were obtained in three independent experiments.

Molecular Modeling of MRS5543 Docking at Human A_3R and $A_{2A}R$. The putative binding conformations of MRS5543 *cis* and *trans* isomers in complex with A_3R and $A_{2A}R$ were evaluated through molecular modeling studies. In particular, a recently reported agonist-bound human $A_{2A}R$ crystallographic structure (PDB ID: 3QAK)[17] and a homology model of the human A_3R,[18] built using this $A_{2A}R$ structure as a template, were used to perform docking simulations of both isomers. The multiply substituted agonist ligand present in this $A_{2A}R$ crystal structure (6-(2,2-diphenylethylamino)-9-((2*R*,3*R*,4*S*,5*S*)-5-(ethylcarbamoyl)-3,4-dihydroxytetrahydrofuran-2-yl)-*N*-(2-(3-(1-(pyridin-2-yl)piperidin-4-yl)ureido)ethyl)-9*H*-purine-2-carboxamide, UK-432097) contained a bulky N^6 substituent, which displaced EL3 to open the binding site and to allow recognition of other N^6 substituted nucleosides.

The docking poses of each MRS5543 isomer inside the A_3R and $A_{2A}R$ binding sites (Figure 6) preserved most of the main receptor−ligand interactions of ribose and adenine moieties

dx.doi.org/10.1021/bc5003373 | Bioconjugate Chem. 2014, 25, 1847−1854

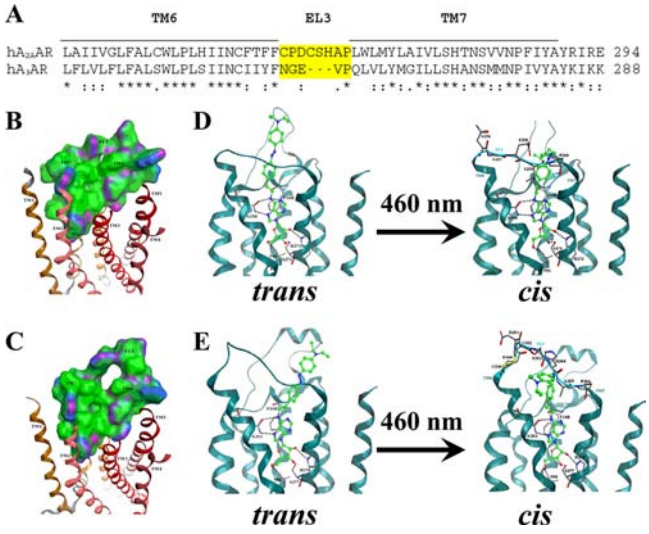

Figure 6. MRS5543 docking at the human A_3R homology model and the human $A_{2A}R$ X-ray structure. (A) Sequence alignment of human $A_{2A}R$ and human A_3R. Sequence of EL3 is highlighted. A detailed view of the region around EL3 of the A_3R (B) and $A_{2A}R$ (C) is shown. The Connolly surface of residues belonging to EL3 and to the upper parts of TM6 and TM7 is displayed. Surface color indicates hydrophobic regions (green), mildly polar regions (blue), and H-bonding regions (magenta). The docking poses of MRS5543 *trans* and *cis* isomers (in green) inside the binding site of the A_3R (D) and $A_{2A}R$ (E) is shown. Side chains of some amino acids important for ligand recognition and H-bonding interactions are highlighted. Hydrogen atoms are not displayed.

observed in the agonist-bound $A_{2A}R$ crystal structures.[17,19] In particular, the 3′- and 2′-hydroxyl groups formed H-bonds with hydrophilic residues (using a GPCR numbering convention)[20] at positions 7.42 (Ser277 in $A_{2A}R$ and Ser271 in A_3R) and 7.43 (His278 in $A_{2A}R$ and His272 in A_3R), respectively. Furthermore, a threonine residue at position 3.36 (Thr88 in $A_{2A}R$ and Thr94 in A_3R) formed a H-bond with the 5′-hydroxymethyl group of the ligand. The side chain of asparagine 6.55 (Asn253 in $A_{2A}R$ and Asn250 in A_3R) strongly interacted with the compound through two H-bonds involving the 6-amino group and the N7 atom of the adenine ring. Moreover, the adenine core was anchored inside the binding site by a $\pi-\pi$ stacking interaction with a phenylalanine in EL2 (Phe168 in $A_{2A}R$ and Phe168 in A_3R) and strong hydrophobic contacts with leucine 6.51 (Leu249 in $A_{2A}R$ and Leu246 in A_3R) and isoleucine 7.39 (Ile274 in $A_{2A}R$ and Ile268 in A_3R). Even though the interactions formed by the two isomers with the residues of the lower part of the ARs binding sites were very similar, some differences were observed when considering the interactions with the upper part of the cavity and the loop region.

As shown in Figure 6, at both the $A_{2A}R$ and A_3R, the N^6 substituent of the MRS5543 *trans* isomer was directed toward the outside of the cavity, and it was predicted to make contact with residues of EL2. However, no significant differences were seen in the interactions of MRS5543 with the two receptor subtypes. In contrast, the N^6-substituent of the *cis* isomer impinged on top of the binding site entrance, and its orientation and interactions were particular for each receptor subtype, mainly due to differences in the residues present in the upper region of the binding sites (Figure 6B,C). Interestingly, at the $A_{2A}R$ structure, the distal *p*-diethylaminophenyl moiety was able to fit a subpocket located under EL3 and between TM6 and TM7, delimited by Ile252 (6.54), Phe255 (6.57), Thr256 (6.58), Pro260 (EL3), Cys262 (EL3), His264 (EL3), Ala265 (EL3), and Met270 (7.35) (Figure 6C,E). On the other hand, at the A_3R structure there was no side pocket between TM6 and TM7 able to accommodate the *p*-diethylaminophenyl group (Figure 6B,D), and this determined a different orientation of the N^6 substituent. This substituent was located more external to the binding cavity and able to adopt different poses (Figure 6D).

In fact, as shown in Figure 6, the region around EL3 at the A_3R is narrower and not suitable to accommodate the N^6 substituent, as compared to that of the $A_{2A}R$, which shows an opening under the loop. This is mainly due to the fact that EL3 of the A_3R is shorter (5 residues long) in comparison to EL3 of the $A_{2A}R$ (8 residues long) (Figure 6A). Moreover, in the $A_{2A}R$ EL3 presents a disulfide bridge (Cys259-Cys262), and two proline residues that confer more rigidity to the loop and potentially stabilize it in a conformation that leads to the formation of the subpocket between TM6 and TM7. Interestingly, mutagenesis studies at the A_1R showed that mutation of the two proline residues in EL3 affects basal activation levels and agonist potency at this subtype, suggesting that rigidity in EL3 is an important feature in receptor activation.[21] Our previous study on a series of 4′-truncated (N)-methanocarba-adenosine derivatives also highlighted the importance of specific interactions of the N^6-substituents with the region located between TM6 and TM7 in determining different affinity and selectivity profiles at ARs.[18] Overall, some differences were observed for the two MRS5543 isomers over A_3R and $A_{2A}R$ subtypes that could be related to structural differences in the EL3 region of these receptors and its ability to interact with the N^6 substituent, thus having potential implications for ligand binding and/or receptor activation.

DISCUSSION

The use of photoisomerizable receptor ligands was first designed for operating with fast ion channels,[22−24] while its application to GPCRs has been much more recent.[6,7] Recently, azobenzene moieties were incorporated into bioactive peptides and cyclopeptides that act through GPCRs as conformational probes to establish relationships with its bioactivity.[25] Here, we synthesized a chemically stable arylazo derivative MRS5543 of a known nonselective adenosine receptor agonist as a pharmacological tool for probing the dependence on receptor affinity and efficacy of conformational effects, particularly by direct contact with the extracellular regions of the receptor. Thus, we fused a commonly used photoisomerizable azobenzene moiety to a known GPCR pharmacophore, i.e., APNEA, with the expectation that it would interact with conformationally sensitive regions of adenosine receptors. The distal azobenzene moiety that was fused also contained a *p*-diethylamino group that increased the reactivity of this moiety toward diazonium salts and the water solubility of the final product, which was not expected to prevent receptor binding. In addition, this substituent also red-shifted the absorption spectrum of the azobenzene unit and decreased the thermal stability of its *cis* isomer, thus enabling operation of the system with visible light and a single irradiation source. Importantly, the N^6 moiety of adenosine receptor agonists is known to be amenable to extensive structural variation while retaining receptor interactions. Moreover, this substituent class is known to associate with a conformationally plastic and potentially functionally

dx.doi.org/10.1021/bc5003373 | *Bioconjugate Chem.* 2014, 25, 1847−1854

important region of adenosine receptors. On the other hand, we used an X-ray structure of the A_{2A} receptor and a well-validated homology model of the closely related A_3 receptor to predict differential interactions of *cis* and *trans* isomers. By basing the design of MRS5543 on APNEA, it was possible to achieve high affinity of the diazo derivative at both A_{2A} and A_3 receptors.

Evidence is increasing that plasticity of the ELs may have implications for the activation of GPCRs. Interestingly, here we characterized the effects of distinct *cis* and *trans* isomers of this nucleoside on the adenylyl cyclase system. However, the effects on other effector systems that may be coupled to these adenosine receptor subtypes are unknown and would not necessarily follow the same characteristic patterns we revealed. For instance, it is known that APNEA exerts A_{2A}R-dependent effects in rat cortical synaptosomes through N-type calcium channels.[26] However, it is not known whether isomers of MRS5543 would exert differential effects in that model. Also, we did not evaluate the effects at the A_1 or A_{2B} receptors; APNEA binds with moderate affinity to the A_1 but not to A_{2B} receptors.[27,28] Therefore, although we were able to provide detailed information on A_3R and A_{2A}R activity, it is necessary to be aware that more work is still needed to elucidate a detailed understanding of the recognition of *cis* and *trans* stereoisomers of MRS5543 at adenosine receptor subtypes in both activated and basal states.

In conclusion, we presented here the first photochromic adenosine-based compound, a visible (less harmful) light-switchable, azobenzene-containing adenosine receptor ligand whose intrinsic activity is light-moldable. The design strategy for this compound was facilitated and results interpreted with the aid of a recently determined X-ray structure of an adenosine receptor. With the surge of new X-ray structures reported for GPCRs,[36] it seems reasonable that similar approaches could be used for many other receptors (GPCRs), which are indeed the mechanistic framework for many of the pharmaceuticals on the market. Accordingly, our application of ligand photomodulation to this important class of signaling proteins, demonstrating the feasibility of modulating metabotropic receptors by small molecules using light, could serve as a model for a much broader application of this kind of approach. We envision its application both in pharmacological tool compounds and potentially in therapeutic agents toward the goal of achieving a site- and time-specific action.

EXPERIMENTAL PROCEDURES

Synthesis of MRS5543. All reagents and solvents were purchased from Sigma-Aldrich (St. Louis, MO, USA). ^{1}H NMR spectra were obtained with a Bruker 400 spectrometer (Bruker Corp., Billerica, MA, USA), and chemical shifts are expressed in δ values (ppm) with tetramethylsilane (δ 0.00). Analytical TLC was performed using glass sheets precoated with silica gel F254 (0.2 mm) from Sigma-Aldrich. The purity of final nucleoside derivative was shown to be >95% (detection at 254 nm) using a Hewlett−Packard 1100 HPLC equipped with a Zorbax SB-Aq 5 μm analytical column (50 × 4.6 mm; Agilent Technologies Inc., Palo Alto, CA, USA). Mobile phase: linear gradient solvent system, 5 mM TBAP (tetrabutylammonium dihydrogen phosphate)−CH_3CN from 80:20 to 0:100 in 13 min; the flow rate was 0.5 mL/min. Peaks were detected by UV absorption with a diode array detector at 230, 254, and 280 nm.

N^6-2-(4-{(*E*)-[4-(Diethylamino)phenyl]diazenyl}phenyl)-ethyladenosine (MRS5543, **2**) was synthesized as follows (Figure 1). APNEA (10 mg, 25.8 μmol, **1**) was dissolved in hydrochloric acid solution (20% of 12 M hydrochloric acid in water; 200 μL) and the solution cooled to 0 °C using an ice bath with vigorous stirring. A solution of sodium nitrite (2.0 mg; 28 μmol) in water (10 μL) was then added and the solution stirred at 0 °C for 20 min to allow formation of the diazonium salt to occur (Figure 1, step 1). During this time, *N*,*N*-diethylaniline (5.0 μL; 33 μmol) (Figure 1) dissolved in methanol (5 μL) and sodium hydroxide (10% soln. in water; 200 μL) (Figure 1, step 2) was cooled to 0 °C. This solution was then added dropwise to the preformed, cooled diazonium salt solution in the dark, and the solution was adjusted to neutrality. The solution was extracted with ethyl acetate (10 mL); the organic layer was separated, washed with saturated aqueous sodium bicarbonate solution (2 × 10 mL) and brine (1 × 10 mL), dried ($MgSO_4$), and then concentrated under reduced pressure to give a yellowish brown solid. This solid was purified by semipreparative silica gel plate chromatography (5:1 dichloromethane: methanol). Evaporation of the solvents provided the title compound as a homogeneous yellow solid (7 mg, 50%). δ_H (CD_3CN): 8.26 (1H, bs), 7.97 (1H, bs), 7.79 (2H, d, J = 9.24 Hz), 7.73 (2H, d, J = 8.4 Hz), 7.42 (2H, d, J = 8.04 Hz), 6.82 (2H, d, J = 9.28 Hz), 5.8 (1H, d, J = 6.88 Hz), 4.82−4.79 (1H, m), 4.32−4.31 (1H, m), 4.16 (1H, m), 3.9 (2H, bm), 3.83−3.79 (1H, m), 3.69−3.64 (1H, m), 3.49 (4H, q), 3.07 (2H, t), 1.21 (6H, t). HRMS: (MH+) found 547.2781; $C_{28}H_{35}O_4N_8$ requires 547.2759.

Photochemical Characterization of MRS5543. Steady-state absorption measurements were registered in a UV−vis HP 8453 spectrophotometer (Agilent Technologies, Inc., Colorado Springs, CO, USA). Transient absorption measurements were performed by means of a LKII laser flash photolysis spectrometer (Applied Photophysics, Surrey, UK) equipped with a Xe lamp, a monochromator, and a photomultiplier (PMT) tube (Hamamatsu Photonics, Hamamatsu, Japan). The 20 ns pulsed laser beam arising from an Rainbow OPO (Quantel, Les Ulis, France) pumped by a Nd:YAG Brilliant laser (Quantel) was used to excite the solutions of interest at 460 nm and 1 mJ/p. The signal from the PMT tube was collected in a 500 MHz oscilloscope (Agilent Technologies, Inc.) and transferred to an Accorn PCRisk station. In this way the decay kinetics of photogenerated transient species at selected wavelengths could be measured and subsequently analyzed by means of nonlinear least-squares exponential fittings.

Plasmid Constructs. The use of the $A_{2A}R^{Rluc}$ was previously described,[29] and the A_3R^{Rluc} construct was obtained using standard molecular biology techniques and the cDNA encoding the human A_3R gene as a template.[30] Briefly, the human A_3R sequence was amplified using the sense oligonucleotide primer FA3*Xho*I (5′-CGGCTCGAGATG-CCCAACAACAGCACTGCTC-3′) and the antisense primer RA3*Bam*HI (5′-GCGGGATCCCGCTCAGAATTCTTC-TCAATGCTTGTGTCC-3′). The fragment was then subcloned in-frame into the *Xho*I/*Bam*HI sites of the pRluc-N1 (Packard Bioscience, Madrid, Spain), resulting in the A_3R with *Renilla* luciferase at its C-terminus (A_3R^{Rluc}). All constructs were verified by nucleotide sequencing.

Cell Culture and Transfection. Human embryonic kidney (HEK-293T) cells were grown in Dulbecco's modified Eagle's medium (DMEM) (Sigma-Aldrich) supplemented with 1 mM sodium pyruvate, 2 mM L-glutamine, 100 μg/mL streptomycin, 100 U/mL penicillin, and 5% (v/v) fetal bovine serum at 37 °C

and in an atmosphere of 5% CO_2. Cells were transiently transfected with TransFectin Lipid Reagent (Bio-Rad Laboratories, Hercules, CA, USA).

MTT Viability Assay. The impact of MRS5543 treatment and 460 nm irradiation on cell viability was examined by MTT assay. In brief, HEK-293T cells were grown in 96-well plates for 24 h. Cells were treated during 2 h with increasing concentrations of MRS5543 with and without irradiation at 460 nm by using a custom-made 9 × 4 light-emitting diode (LED) matrix (12 × 9 cm) (FCTecnics, Barcelona, Spain) installed in the culture hood at height of 2 cm above the cells. Subsequently, the cells were washed and incubated for 2 h in the dark at 37 °C with 3-(4,5-dimethylthiazol-2-yl)-2,5-diphenyltetrazolium bromide (MTT) (Sigma-Aldrich). Following the lysis of the cells the cell viability was determined by measuring the absorbance at 560 nm. Interestingly, the MRS5543 treatment (ranging from 10 nM to 3.3 μM) did not affect the cell viability in either dark or upon 460 nm irradiation conditions (Supporting Information Figure 1).

cAMP Assay. We used a dual luciferase reporter assay to indirectly detect variations of cAMP levels in transiently transfected HEK-293T cells. Accordingly, cells were seeded at a density of 1 × 10^6 cells/well in 6-well dishes, and co-transfected with 2 μg of the plasmid encoding the cAMP response element−firefly luciferase fusion protein (pGL4-CRE-luc2p; Promega, Madison, WI, USA) plus 2 μg of plasmid encoding either $A_{2A}R^{Rluc}$ or A_3R^{Rluc}, approximately 36 h after transfection and then treatment with the indicated ligand during 2 h in the presence of 50 μM zardaverine and with and without irradiation at 460 nm. Cells were then harvested, washed twice with PBS, and the firefly luciferase luminescence (FLU) determined using the Bright-Glo luciferase assay system (Promega) following the manufacture's indications. The *Renilla* luciferase luminescence (RLU) was determined by incubating the cells with 5 μM of benzyl-coelenterazine (NanoLight Technology, Pinetop, AZ, USA).[31] Both firefly and *Renilla* luminescence was measured in a POLARstar Optima plate reader (BMG Labtechnologies, Ortenberg, Germany) using a 30 nm bandwidth 535 nm filter setting. The firefly luciferase activity was normalized against *Renilla* luciferase values (i.e., FLU/RLU) for each data point.

Statistics. The number of samples (n) in each experimental condition is indicated in the figure legends. The statistical analysis was performed by two-way analysis of variance (ANOVA) followed by Bonferroni posthoc test. Statistical significance was set as $P < 0.05$.

Molecular Modeling. The adenosine derivatives (prepared for docking using the build panel and the LigPrep panel implemented in the Schrödinger suite)[32] were docked in an agonist-bound structure of the human $A_{2A}R$ (PDB code 3QAK)[17] and in a model of the closely related human A_3R. More precisely, a model of the $h_{A2}AR$ was built, using the homology modeling tool implemented in the MOE suite,[33] to fill the portion of EL2 that is missing in the crystal (from Gly142 to Leu167). Coordinates for these residues were taken from another agonist-bound $hA_{2A}R$ crystal structure (PDB code 2YDV).[19] The human A_3R homology model was built using MOE suite,[33] as previously reported,[18,34] based on the human $A_{2A}R$ structure[17] as a template.

Glide[35] module of the Schrödinger suite was used for the docking in the rigid binding site using the SP (standard precision) procedure. A Glide Grid was centered within key conserved residues of the binding pocket, i.e., Phe (EL2), Asn (6.55), Trp (6.48), and His (7.43). The Glide Grid was built using an inner box (ligand diameter midpoint box) of 6 Å × 6 Å × 14 Å and an outer box that extended 20 Å in each direction from the inner one. The top scoring docking poses for each ligand were subjected to visual inspection and analysis of protein−ligand interactions to select the proposed binding conformations.

■ ASSOCIATED CONTENT

Supporting Information

Additional figure. This material is available free of charge via the Internet at http://pubs.acs.org.

■ AUTHOR INFORMATION

Corresponding Authors

*E-mail: kennethj@helix.nih.gov.
*E-mail:pau@icrea.cat.
*E-mail: fciruela@ub.edu.

Author Contributions

María Isabel Bahamonde, Jaume Taura, and Silvia Paoletta contributed equally.

Notes

The authors declare no competing financial interest.

■ ACKNOWLEDGMENTS

This work was supported by grants SAF2011-24779, CTQ2012-30853, PCIN-2013-019-C03-03 and Consolider-Ingenio CSD2008-00005 from "Ministerio de Economía y Competitividad" (MINECO) and ICREA Academia-2010 from the Catalan Institution for Research and Advanced Studies (ICREA) to FC. Also, V.F.-D., J.T., and F.C. belong to the "Neuropharmacology and Pain" accredited research group (Generalitat de Catalunya, 2014 SGR 1054) and P.G. belongs to the "Bioelectrochemistry and nanotechnology" accredited research group (Generalitat de Catalunya, 2014 SGR 1251). Support to K.A.J., S.P., A.A.G., and S.C. from the NIDDK Intramural Research Program of the National Institutes of Health, Bethesda, MD, USA is acknowledged. Also, support to AAG from the Discovery Chemistry Project funded in part by the U.S. Department of Energy in collaboration with the National Cancer Institute is acknowledged. MIB acknowledges postdoctoral fellowships from the Beatriu de Pinós (Generalitat de Catalunya) and Marie Curie (European Union) programs. This project has received funding from the European Union's Seventh Framework Programme for research, technological development and demonstration under grant agreement numbers 270483 (Focus), 210355 (Opticalbullet), and 335011 (Theralight). We are also grateful to the RecerCaixa foundation (2010ACUP00378) and the Marató de TV3 foundation (111531).

■ REFERENCES

(1) Snyder, S. H. (1985) Adenosine as a neuromodulator. *Annu. Rev. Neurosci. 8*, 103−124.
(2) Palmer, T. M., and Stiles, G. L. (1995) Adenosine receptors. *Neuropharmacology 34*, 683−694.
(3) Jacobson, K. A., and Gao, Z. G. (2006) Adenosine receptors as therapeutic targets. *Nat. Rev. Discovery 5*, 247−264.
(4) Mourot, A., Kienzler, M. A., Banghart, M. R., Fehrentz, T., Huber, F. M. E., Stein, M., Kramer, R. H., and Trauner, D. (2011) Tuning photochromic ion channel blockers. *ACS Chem. Neurosci. 2*, 536−43.
(5) Kano, K., Tanaka, Y., Ogawa, T., Shimomura, M., and Kunitake, T. (1981) Photoresponsive artificial membrane Regulation of

membrane permeability of liposomal membrane by photoreversible cis-trans isomerization of azobenzenes. *Photochem. Photobiol. 34*, 323−329.
(6) Levitz, J., Pantoja, C., Gaub, B., Janovjak, H., Reiner, A., Hoagland, A., Schoppik, D., Kane, B., Stawski, P., Schier, A. F., Trauner, D., and Isacoff, E. Y. (2013) Optical control of metabotropic glutamate receptors. *Nat. Neurosci. 16*, 507−16.
(7) Pittolo, S., Gómez-Santacana, X., Eckelt, K., Rovira, X., Dalton, J., Goudet, C., Pin, J.-P., Llobet, A., Giraldo, J., Llebaria, A., and Gorostiza, P. A photochromic allosteric modulator to control an endogenous G protein-coupled receptor with light. *Nat. Chem. Biol.*, In press.
(8) Gorostiza, P., and Isacoff, E. Y. (2008) Optical switches for remote and noninvasive control of cell signaling. *Science 322*, 395−9.
(9) Tchilibon, S., Kim, S.-K., Gao, Z.-G., Harris, B. A., Blaustein, J. B., Gross, A. S., Duong, H. T., Melman, N., and Jacobson, K. A. (2004) Exploring distal regions of the A_3 adenosine receptor binding site: sterically constrained N6-(2-phenylethyl)adenosine derivatives as potent ligands. *Bioorg. Med. Chem. 12*, 2021−34.
(10) Chi, L., Sadovski, O., and Woolley, G. A. (2006) A blue-green absorbing cross-linker for rapid photoswitching of peptide helix content. *Bioconjugate Chem. 17*, 670−676.
(11) Izquierdo-Serra, M., Gascón-Moya, M., Hirtz, J. J., Pittolo, S., Poskanzer, K. E., Ferrer, E., Alibés, R., Busqué, F., Yuste, R., Hernando, J., and Gorostiza, P. (2014) Two-photon neuronal and astrocytic stimulation with azobenzene-based photoswitches. *J. Am. Chem. Soc. 136*, 8693−701.
(12) Khalaf, A. I., Anthony, N., Breen, D., Donoghue, G., Mackay, S. P., Scott, F. J., and Suckling, C. J. (2011) Amide isosteres in structure-activity studies of antibacterial minor groove binders. *Eur. J. Med. Chem. 46*, 5343−55.
(13) Bandara, H. M. D., and Burdette, S. C. (2012) Photoisomerization in different classes of azobenzene. *Chem. Soc. Rev. 41*, 1809−25.
(14) Schanze, K. S., Mattox, T. F., and Whitten, D. G. (1983) Solvent effects on the thermal cis-trans isomerization and charge-transfer absorption of 4-(diethylamino)-4′-nitroazobenzene. *J. Org. Chem. 48*, 2808−2813.
(15) Fozard, J. R., and Carruthers, A. M. (1993) Adenosine A_3 receptors mediate hypotension in the angiotensin II-supported circulation of the pithed rat. *Br. J. Pharmacol. 109*, 3−5.
(16) Palmer, T. M., Gettys, T. W., and Stiles, G. L. (1995) Differential interaction with and regulation of multiple G-proteins by the rat A_3 adenosine receptor. *J. Biol. Chem. 270*, 16895−902.
(17) Xu, F., Wu, H., Katritch, V., Han, G. W., Jacobson, K. A., Gao, Z.-G., Cherezov, V., and Stevens, R. C. (2011) Structure of an agonist-bound human A_{2A} adenosine receptor. *Science 332*, 322−7.
(18) Tosh, D. K., Paoletta, S., Deflorian, F., Phan, K., Moss, S. M., Gao, Z.-G., Jiang, X., and Jacobson, K. A. (2012) Structural sweet spot for A_1 adenosine receptor activation by truncated (N)-methanocarba nucleosides: receptor docking and potent anticonvulsant activity. *J. Med. Chem. 55*, 8075−90.
(19) Lebon, G., Warne, T., Edwards, P. C., Bennett, K., Langmead, C. J., Leslie, A. G., and Tate, C. G. (2011) Agonist-bound adenosine A_{2A} receptor structures reveal common features of GPCR activation. *Nature 474*, 521−525.
(20) Ballesteros, J. A., and Weinstein, H. (1995) Integrated methods for the construction of three-dimensional models of structure−function relations in G protein-coupled receptors. *Methods Neurosci. 25*, 366−428.
(21) Peeters, M. C., Wisse, L. E., Dinaj, A., Vroling, B., Vriend, G., and Ijzerman, A. P. (2012) The role of the second and third extracellular loops of the adenosine A1 receptor in activation and allosteric modulation. *Biochem. Pharmacol. 84*, 76−87.
(22) Banghart, M., Borges, K., Isacoff, E., Trauner, D., and Kramer, R. H. (2004) Light-activated ion channels for remote control of neuronal firing. *Nat. Neurosci. 7*, 1381−6.
(23) Volgraf, M., Gorostiza, P., Numano, R., Kramer, R. H., Isacoff, E. Y., and Trauner, D. (2006) Allosteric control of an ionotropic glutamate receptor with an optical switch. *Nat. Chem. Biol. 2*, 47−52.
(24) Bartels, E., Wassermann, N. H., and Erlanger, B. F. (1971) Photochromic activators of the acetylcholine receptor. *Proc. Natl. Acad. Sci. U. S. A. 68*, 1820−3.
(25) Renner, C., and Moroder, L. (2006) Azobenzene as conformational switch in model peptides. *ChemBioChem 7*, 868−78.
(26) Li, S. N., and Wong, P. T. (2000) The adenosine receptor agonist, APNEA, increases calcium influx into rat cortical synaptosomes through N-type channels associated with A2a receptors. *Neurochem. Res. 25*, 457−9.
(27) Olah, M. E., and Stiles, G. L. (1995) Adenosine receptor subtypes: characterization and therapeutic regulation. *Annu. Rev. Pharmacol. Toxicol. 35*, 581−606.
(28) Alexander, S. P., Cooper, J., Shine, J., and Hill, S. J. (1996) Characterization of the human brain putative A_{2B} adenosine receptor expressed in Chinese hamster ovary (CHO.A2B4) cells. *Br. J. Pharmacol. 119*, 1286−90.
(29) Ciruela, F., Burgueno, J., Casado, V., Canals, M., Marcellino, D., Goldberg, S. R., Bader, M., Fuxe, K., Agnati, L. F., Lluis, C., Franco, R., Ferre, S., and Woods, A. S. (2004) Combining mass spectrometry and pull-down techniques for the study of receptor heteromerization. Direct epitope-epitope electrostatic interactions between adenosine A_{2A} and dopamine D_2 receptors. *Anal. Chem. 76*, 5354−5363.
(30) Salvatore, C. A., Jacobson, M. A., Taylor, H. E., Linden, J., and Johnson, R. G. (1993) Molecular cloning and characterization of the human A_3 adenosine receptor. *Proc. Natl. Acad. Sci. U. S. A. 90*, 10365−10369.
(31) Gandía, J., Fernández-Dueñas, V., Morató, X., Caltabiano, G., González-Muñiz, R., Pardo, L., Stagljar, I., and Ciruela, F. (2013) The Parkinson's disease-associated GPR37 receptor-mediated cytotoxicity is controlled by its intracellular cysteine-rich domain. *J. Neurochem. 125*, 362−72.
(32) *Schrödinger Suite 2012*, Schrödinger, LLC, New York, USA.
(33) *Molecular Operating Environment (MOE)*, v 2012.10, Chemical Computing Group Inc, Montreal, Canada.
(34) Tosh, D. K., Deflorian, F., Phan, K., Gao, Z.-G., Wan, T. C., Gizewski, E., Auchampach, J. A., and Jacobson, K. A. (2012) Structure-guided design of A_3 adenosine receptor-selective nucleosides: combination of 2-arylethynyl and bicyclo[3.1.0]hexane substitutions. *J. Med. Chem. 55*, 4847−60.
(35) Friesner, R. A., Banks, J. L., Murphy, R. B., Halgren, T. A., Klicic, J. J., Mainz, D. T., Repasky, M. P., Knoll, E. H., Shelley, M., Perry, J. K., Shaw, D. E., Francis, P., and Shenkin, P. S. (2004) Glide: a new approach for rapid, accurate docking and scoring. 1. Method and assessment of docking accuracy. *J. Med. Chem. 47*, 1739−49.
(36) Costanzi, S., and Wang, K. (2014) The GPCR Crystallography boom: providing an invaluable source of structural information and expanding the scope of homology modeling. *Adv. Exp. Med. Biol. 796*, 3−13.